Time and Spatial Analysis of Flood Disaster based on GPS Data:
A Case Study of Flood Disaster in Nagano City in 2019

楊 一帆[1]，大平 尚輝[1]，郷右近 英臣[1]

Yifan YANG[1], Naoki OHIRA[1], and Hideomi GOKON[1]

[1] 北陸先端科学技術大学院大学 先端科学技術研究科

This paper presents a case study of a flood disaster in Nagano City in 2019, conducting a flood analysis utilizing GPS data. The time and spatial changes of the flood disaster are studied by filtering, classifying, and overlaying GPS data from October 12th to October 14th, 2019, in combination with precipitation and river water level data The study results indicate that there is a correlation between the time of occurrence of GPS abnormal data and the occurrence of flood disaster, and there is also a correlation between the distribution of GPS abnormal data and the flood area during the flood. This study demonstrates the significance and practicality of GPS data in flood disaster analysis, providing valuable insights for enhancing flood disaster response capabilities and urban planning.

Keywords: *Flood Disaster, GPS data, Nagano City, Time and spatial Analysis, Disaster Management*

1. Background

Flood, as one of the most common and devastating natural disasters[1], inflicts significant losses and impacts on human society[2]. Many cities worldwide are under the threat of flood disasters, and Japan, as a country in the East Asian monsoon region, is particularly vulnerable to extreme weather such as typhoons and heavy precipitation[3,4].

In October 2019, the Typhoon Hagibis had severe consequences, including torrential rains, floods, and landslides, causing extensive damage to house and roads[5]. The heavy precipitation from the typhoon resulted in the collapse of the riverbanks along the Chikuma River in Nagano City, leading to severe flooding in the surrounding areas[6] and posing significant challenges to rescue and recovery efforts[7].

When this kinds of large scale flood strikes, the information and communication networks might be disrupted, resulting in a lack of information of the affected areas[8]. This situation makes it difficult to evaluate where and what kind of damage has occurred and causes delays in disaster response[9]. To overcome this difficulty, satellite remote sensing technologies have been developed to assess damage in flooded areas using satellite images (e.g., Mohamed, 2019; Skakun *et al.*, 2014; Tariq *et al.*, 2021; Tellman *et al.*, 2021[10]–[13]). However, because satellites have a return period, it is sometimes difficult to immediately assess the situation of the affected area[14].

In this study, we focused on the GPS (Global Positioning System) installed in smartphones. With smartphone GPS data, people flow can be estimated in near real-time[15]. On the other hand, in flooded areas, there is a possibility of losing information on the GPS of the victims' cell phones[16]–[18]. In this study, we considered the possibility of using this principle to estimate the flood area. In recent years, with the continuous development and widespread application of GPS technology, this technology has gained increasing attention in the field of natural disasters[19]. Compared to conventional methods using satellites and drones[20], GPS data offers unique advantages in flood disaster monitoring[21]. Providing high-precision spatial and temporal information, GPS data offers new perspectives and methods for analyzing and researching flood disasters[22]. Utilizing GPS data for flood disaster analysis allows for a more accurate understanding of the propagation path[23], and this information may provide valuable information for the flood area[24,25], and the impact of floods[26], thereby aiding the formulation of effective response measures and post-disaster recovery plans. Furthermore, the near real-time nature of GPS data enables monitoring the evolving process of floods[27], offering crucial disaster information for timely emergency response and decision-making support[28]. Therefore, the application of GPS data in flood disaster time analysis holds significant academic value and practical significance, offering assistance in improving flood disaster response capabilities and urban planning[29].

While it would be a useful technology to predict the flood area based on changes in the number of GPS complements[30], a challenge makes this problematic: the location information obtained from the GPS is very limited and fragmentary[31]. To obtain GPS information, the smartphone GPS function must be set up in advance so that the data can be retrieved, but many users of mobile phones turn off the functionality of their phones[32]. Therefore, we need to think of a method to estimate the flood area from a limited number of GPS locations.

Towards this orientation, this paper aims to use GPS data to conduct a time and spatial analysis of the 2019 flood disaster in Nagano City. Explore the impact of GPS data on the city and its disaster prevention significance, thereby providing valuable insights for enhancing flood disaster response capabilities and urban planning. The study findings are expected to offer flood disaster management recommendations for Nagano City and other potentially affected regions, ultimately strengthening the city's resilience against natural disasters.

2.   Research Area and Research Data

（1）Research Area

As shown in Figure 1, the research area of this paper is Nagano City, located in the central part of Honshu Island, Japan. Nagano City serves as the capital city of Nagano Prefecture and is the largest and most populous city in the prefecture. The convergence of the Chikuma River and the Sai River in Nagano City brings abundant natural resources but also makes it susceptible to disasters such as floods.

The main objective of this study is to conduct a comprehensive analysis of flood disaster of Nagano City in 2019 in time and spatial. As shown in Figure 2, 189 administrative districts were selected from a total of 433 districts in Nagano City, with an average elevation of 380 meters or below, to accurately study the low-lying areas at higher risk of flooding.

（2）Research Data

The research data includes precipitation and river water level data for Nagano City from October 12th to October 14th, 2019, as obtained from the Ministry of Land, Infrastructure, Transport, and Tourism of Japan, as shown in Figure 3. The research period is selected from October 12th to October 14th, 2019, during which October 12th experienced heavy rainfall in Nagano City, and from the 12th to the 14th, the Chikuma River embankments collapsed, and floods occurred.

GPS location data were collected from a smartphone application provided by   Agoop Corp. The data underwent of location information. The anonymous nature of the data anonymization and statistical processing to form a large dataset prevents the identification of specific individuals' locations but reflects the overall population's positional changes. There are a total of 26 fields in these data, and this study uses a total of 12 fields as shown in Table 1.
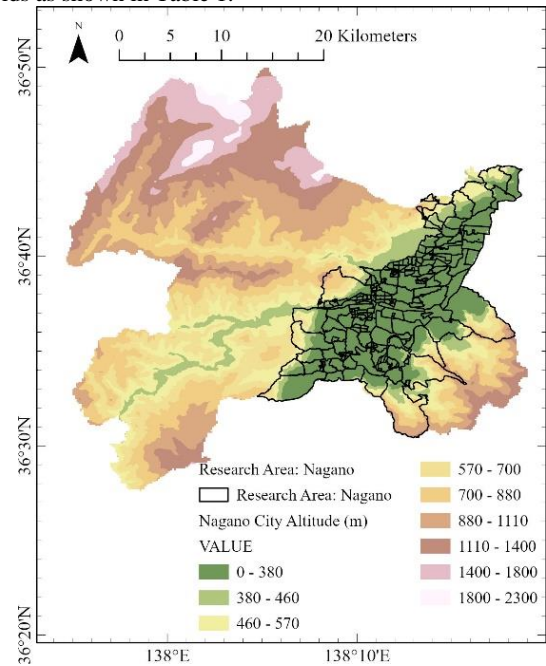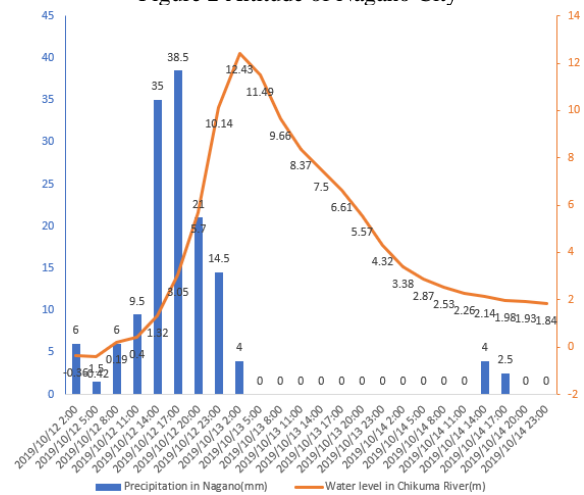

Figure 2 Altitude of Nagano City

Figure 3 Precipitation data in Nagano City and water level data in Chikuma River

Table 1 GPS data fields

Data field	Data interpretation
dailyid	User daily ID
year	Year
month	Month
day	Day
dayofweek	Day of week
hour	Hour
minute	Minute
latitude	Latitude
longitude	Longitude
accuracy	GPS Accuracy
prefcode	Prefecture code
citycode	City/town/village code

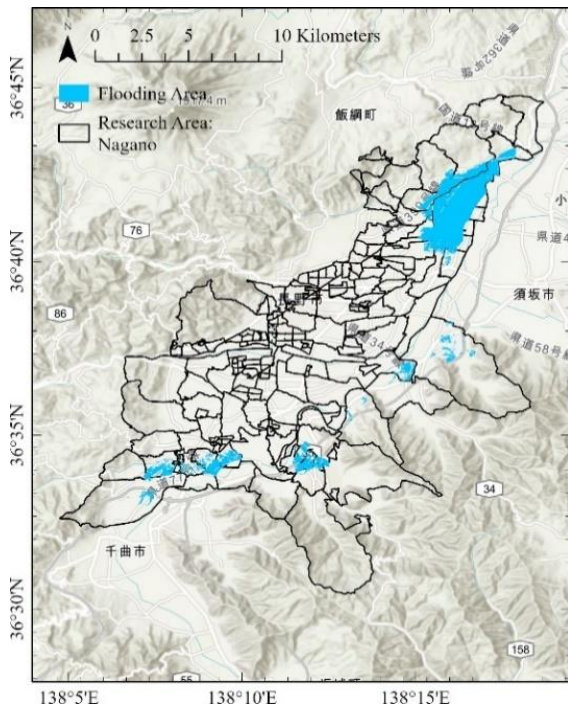Figure 1 Location of Nagano City

Figure 4 flood area in Nagano City

Furthermore, the basic boundary data of Nagano City and the flood disaster extent data, as shown in Figure 4, were obtained from the website of the Ministry of Land, Infrastructure, Transport, and Tourism of Japan.

Through the analysis of the above data, this study aims to delve into and analyze the correlation between flood disasters and GPS data changes.

3. Research Method

（1）Data Selection and Processing

Data from October 12th to October 14th, 2019, were selected from the data source. The data corresponding to Nagano City was selected based on its specific data code (20201). As the research area encompasses administrative districts in Nagano City with elevations below 380 meters, the data was visualized using ArcGIS Pro to extract the data within the geographical extent of the research area.

（2）Data Accuracy Processing

The accuracy of GPS data is measured in meters (m), indicating the potential location within a circle centered at the given point with the accuracy as its radius. According to information released by Agoop Corp., the accuracy of GPS data is approximately 70%. Setting the precision threshold to 100 meters results in retaining approximately 70% of the total data. In order to ensure data quality, the accuracy threshold is set at 100m, and data with an accuracy exceeding 100m will be excluded. This is mathematically represented as:
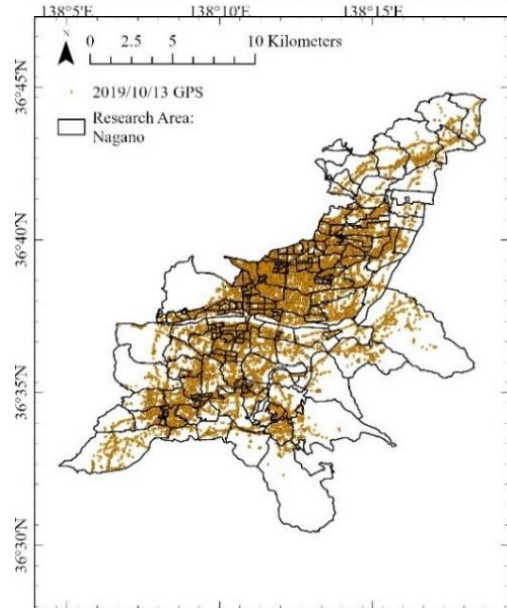
Processed dataset = { GPS data | $accuracy \leq 100$ }　　　[1]

The distribution of processed GPS data for each day is shown in Figure 5.

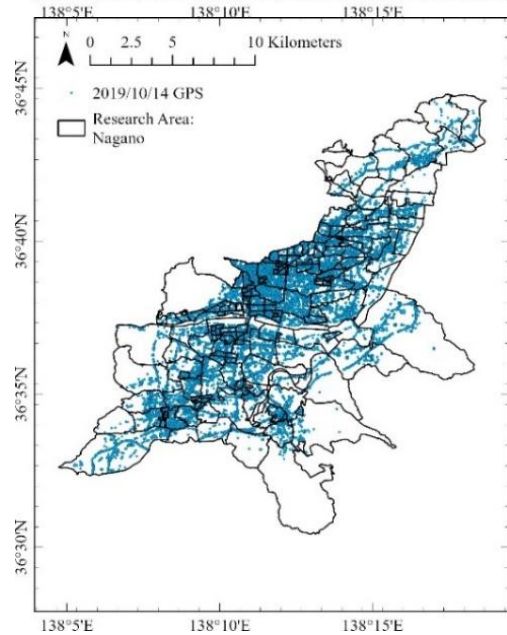2019/10/12
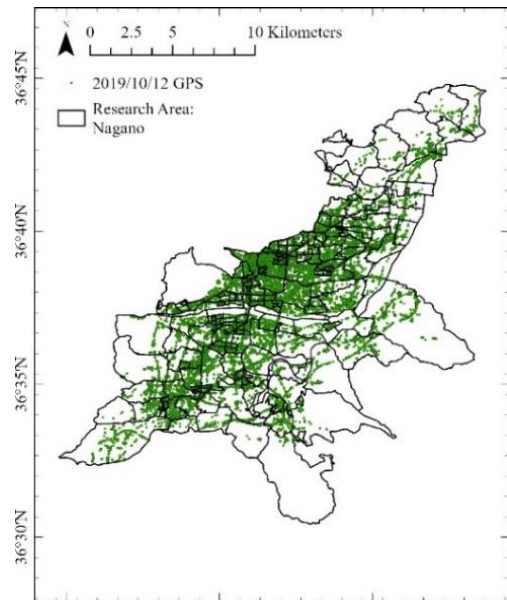
2019/10/13

2019/10/14

Figure 5 GPS data distribution map

Figure 6 shows the GPS data amount for each hour from October 12th, 2019, to October 14th, 2019. It can be observed that there is no significant variation in the overall GPS data volume daily. GPS data is generated in real-time based on the movement of the location; when there is no movement, the position information is only periodically updated. Therefore, the GPS data volume is relatively low at night, partly because some individuals turn off their phones while sleeping, and primarily because most people do not change their positions during the night. The stability daily and the variability on an hourly basis of this data demonstrate its ability to accurately reflect population movement, indicating a certain level of accuracy.

（3）Data Classification

The total duration of the study is 3 days, totaling 72 hours. To observe the changes in the GPS data, the three days are divided into 12 evenly spaced time intervals, each spanning 6 hours. This division of time provides sufficient spatial and temporal resolution to quickly determine the time period and date of the flood.

Let D represent the GPS data set. Each time interval is 6 hours long and can be represented as follows:

$$D = \{ D_1, D_2, ..., D_{12} \} \qquad [2]$$

D_1 represents the GPS data set for the first six-hour interval, D_2 represents the GPS data set for the second six-hour interval, and so on until D_{12} represents the GPS data set for the twelfth six-hour interval. Table 2 shows the amount of GPS data points in each classified dataset.

（4）Constructing Geographic Grid

To delve into the temporal and spatial changes in GPS data, a geographic grid construction approach was employed. The construction process took into consideration grids of varying specifications with side lengths of 100m, 300m, and 500m, and the quantity of grids for each specification is detailed in Table 3. Through hourly statistical analysis of GPS data from October 12th to 14th, 2019, it was identified that the time interval, with the least GPS data occurred from 3:00 to 4:00 on October 14th, registering only 5331 data points. This count was below the quantity of grids with 100m and 300m side lengths. To maintain data accuracy while avoiding overly sparse or dense data distribution, a decision was made to opt for a grid with a 500m side length, totaling 1222 grids, serving as the fundamental unit for our study.

（5）Data Overlay

Using "Spatial Join" in ArcGIS Pro, the GPS data for each six-hour time interval was overlaid onto the corresponding grid cells, and the "Join Count", representing the number of GPS data points in each grid cell, was calculated. The formula is represented as follows:

$$C = \text{Spatial Join} （D, R） \qquad [3]$$

D represents the GPS data set, R represents the geographic grid data set, and Spatial Join (D, R) refers to overlaying the GPS data set onto the grid data set R and calculating the GPS data count for each grid cell C.

Additionally, the flood area for Nagano City obtained from the website of the Ministry of Land, Infrastructure, Transport, and Tourism of Japan, and it was overlaid onto the grid cells to create the flood grid data as shown in Figure 7, which would be used for subsequent analysis of flood time and area.
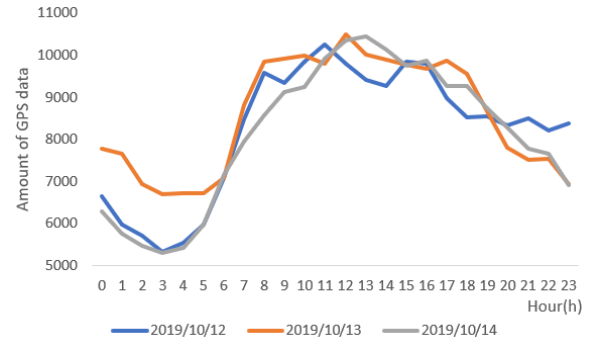

Figure 6 Amount of GPS data amount per hour

Table 2 Amount of GPS data in dataset

Dataset	Amount of GPS data	Dataset	Amount of GPS data
D_1	34538	D_7	60705
D_2	53717	D_8	48939
D_3	56220	D_9	34295
D_4	49757	D_{10}	52113
D_5	42735	D_{11}	59942
D_6	56446	D_{12}	48669

Table 3 Number of grids with different side lengths

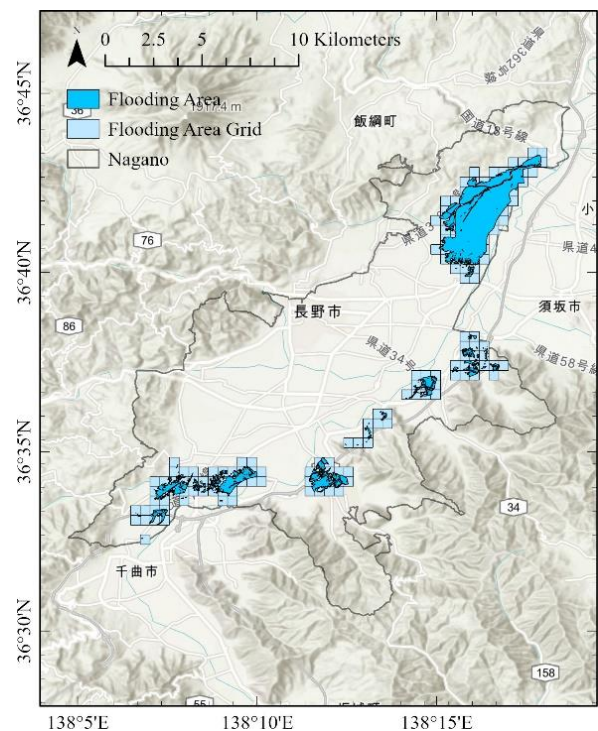| Length	Number of grids
100m	56,400
300m	6,320
500m	1,222

Figure 7 Flood area and flood grids in Nagano City

（6）Overall Analysis of Flood Disaster

Based on the results from 12 time intervals, a comprehensive analysis was conducted on flood disasters and GPS data. This analysis aimed to pinpoint the exact date of the flood occurrence, identify the 6 hours' time interval involved, and approximate flood area. This serves as a crucial reference for subsequent detailed temporal and spatial analyses.

（7）Flood Time Analysis

Based on the overall analysis of the flood disaster, it quantitatively compares the changes in the hourly GPS data, analyzes and determines the time of the flood. Urban population mobility is influenced by various factors, including not only the disaster itself but also seasonal changes, weekdays, and weekends. For example, temperature fluctuations may lead people to prefer indoor activities, and commuting routes during weekdays may differ from those on weekends.

To mitigate the impact of seasonal changes, data from the week before and after the flood were selected for comparative validation. That is, the two weeks from September 29th to October 5th and October 20th to 26th. Simultaneously, to reduce the differences between weekdays and weekends, separate calculations and analyses were conducted.

The data from the week before and the week after the flood were defined as normal date GPS data, while October 12th to 14th, 2019, was considered an abnormal date. Under normal circumstances, the quantity of GPS data fluctuates within a certain range. Any deviation beyond this range indicates abnormal GPS data. In normal conditions, the expected quantity of GPS data at the same time fluctuates within a certain range, which can be modeled by constructing a normal distribution to identify abnormal GPS data.

Specifically, by calculating the mean and standard deviation of the normal distribution of GPS data for each hour in the week before the flood and the second week after the flood occurrence, a mathematical description of the normal distribution of GPS data under normal conditions was obtained. The calculation formulas are as follows:

Normal Distribution: $f(x \mid \mu, \sigma^2) = \frac{1}{\sqrt{2\Pi\sigma^2}} \cdot e^{-\frac{(x-\sigma)^2}{2\sigma^2}}$ [4]

Mean: $\mu = \frac{\sum_{i=1}^{N} x_i}{N}$ [5]

Standard Deviation: $\sigma = \sqrt{\frac{\sum_{i=1}^{N}(x_i - \mu)^2}{N}}$ [6]

N is the number of normal dates and x_i is the number of GPS per i hour.

As 99.7% of data falls within the mean ± 3 standard deviations in a normal distribution, data points outside this expected range are considered outliers. Therefore, by comparing the hourly GPS data for abnormal dates with this range, the time of the flood occurrence can be determined.

The calculation formulas are as follows:

$\begin{cases} \mu - 3\sigma \leq X_i \leq \mu + 3\sigma \\ X_i < \mu - 3\sigma, X_i > \mu + 3\sigma \end{cases} \begin{cases} 0 \\ 1 \end{cases}$ [7]

X_i is the number of GPSs per i hour in the abnormal date, and X_i is assigned a value of 0 if it is in the range and 1 if it is not in the range.

(8) Flood Area Analysis

By quantitatively comparing the changes in GPS data for different grids at different time intervals, the spatial information of GPS data changes was calculated. Through this method, we can identify the geographical areas with abnormally changing GPS data, corresponding to the areas affected by the flood.

Building on the flood event analysis, we calculate the GPS data volume within each grid during the time of flood occurrence. Under normal circumstances, the volume of GPS data for the same grid during the same time interval should also vary within a certain range. An exceeding range indicates abnormal data.

Therefore, a normal distribution model was similarly constructed. Based on the time intervals calculated from the flood event analysis, the mean and standard deviation of the normal distribution of GPS data for each grid was calculated during the week before the flood and the second week after the flood. This provides a mathematical description of the distribution of GPS data under normal conditions. The calculation formulas are as follows:

Normal Distribution: $f(z \mid \mu, \sigma^2) = \frac{1}{\sqrt{2\Pi\sigma^2}} \cdot e^{-\frac{(z-\sigma)^2}{2\sigma^2}}$ [8]

Mean: $\mu = \frac{\sum_{i=1}^{N} z_j}{N}$ [9]

Standard Deviation: $\sigma = \sqrt{\frac{\sum_{i=1}^{N}(z_{i,j} - \mu)^2}{N}}$ [10]

N is the number of normal dates and $z_{i,j}$ is the number of GPS per i hour for the jth grid.

The time ranges of the flood event analysis results were then totaled to get the amount of GPS data for each grid within this time range. The formula is as follows:

$Z_j = \sum_{i=a}^{b} Z_{i,j} \quad (a \leq i \leq b)$ [11]

Z_j is the number of GPSs on the jth grid in the abnormal date within the flood time, a and b are the start and stop times of the flood obtained from the flood time analysis.

Comparing the GPS data for each grid on abnormal dates with this range, if it falls outside the range, it is considered the time of flood occurrence. The calculation formula is as follows:

$\begin{cases} \mu - 3\sigma \leq Z_j \leq \mu + 3\sigma \\ Z_j < \mu - 3\sigma, Z_j > \mu + 3\sigma \end{cases} \begin{cases} 0 \\ 1 \end{cases}$ [12]

Z_j is assigned a value of 0 if it is in the range and 1 if it is not in the range.

For this analysis, refuge shelter data from government website were also downloaded, considering that during flood disasters, people seek refuge in designated shelters based on government notifications. We filtered shelters that were open from October 12th to 14th, 2019, according to government statistical data, to facilitate a spatial analysis of the flood disaster.

4. Result

（1）Overall Variation

Based on the data processing methods described above, GPS data variation charts for 12 time intervals were obtained, as shown in Figure 8.
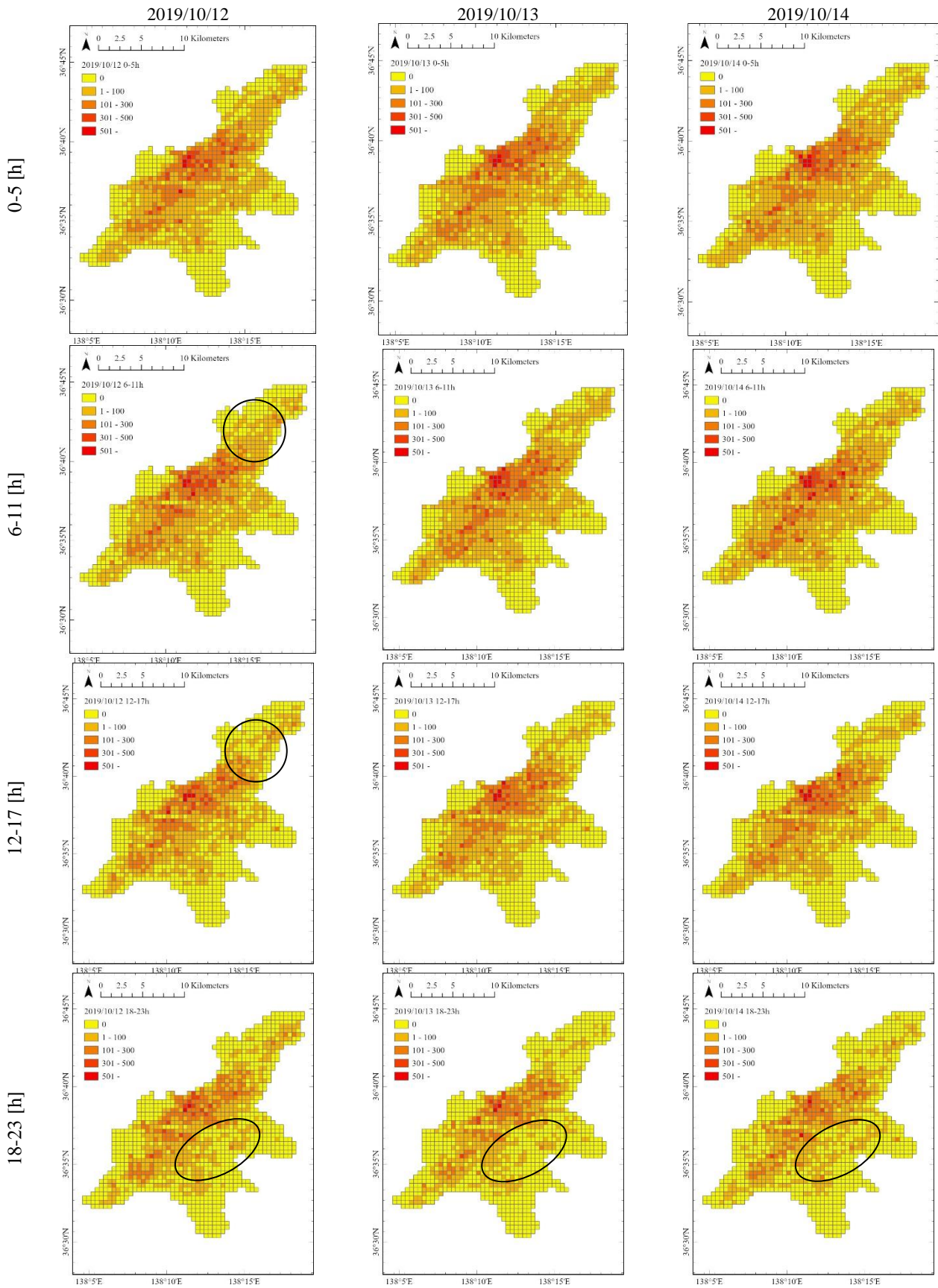
Figure 8 2019/10/12-2019/10/14 GPS Data Variation Chart for Nagano City for 12 Time Intervals

Through the analysis of GPS data charts, it can be observed that, overall, the GPS data variation in the entire research area does not exhibit significant fluctuations. However, comparing the GPS data distribution images from 6:00 to 11:00 and from 12:00 to 17:00 on the 12th, it is obvious that the GPS data in the circled portion of the data in the upper right corner of the data from 12:00 to 17:00 decreases, and that this decrease continues until the 14th, with the most obvious decrease on the 13th.

Meanwhile, comparing the data from 17:00 to 23:00 on the 12th, 13th and 14th, it can be seen that the amount of GPS data in the lower-right circle firstly decreases and then increases, which may indicate that this location was affected by the flood on the 12th and 13th, and recovered on the 14th.

In conclusion, based on the GPS count statistics in Figure 6 and the distribution of GPS counts in Figure 8, as well as the distribution of flood area in Figure 7, it can be seen that there were significant abnormalities in the GPS data in the research area during the flood, and at specific times with specific areas. The results indicate that the flooding occurred mainly on the 12th and 13th day and there is a significant trend of decreasing GPS data in the area associated with the flooding. Therefore, the next temporal and spatial analyses of flood occurrence will focus on the 12th and 13th days.

（2）Time Variation

The overall analysis indicates that the occurrence of the flood was concentrated on October 12th and October 13th, both of which happened to be weekends. In light of this, the focus of the time variation analysis was directed towards the GPS data specifically collected during the weekends.

The detailed results of the time variation analysis are presented in Table 4. In Figure 9, the range between " $\mu + 3\sigma$ " and " $\mu - 3\sigma$ " represents the fluctuation range of GPS counts per hour during a typical weekend under normal circumstances. Notably, the GPS data from 16:00 to 18:30 on October 12th falls below the normal level, while the data from 22:30 to 24:00 on the same day and from 0:00 to 5:00 on the 13th significantly exceed the normal level.

Referring to the precipitation graph in Figure 3, it can be seen that the precipitation in Nagano City during the time period from 16:00 to 18:30 is exceptionally high at 38.5 millimeters, making it the most concentrated period of precipitation for the day. Therefore, it is speculated that the reduced GPS data during this period could be attributed to decreased population movement due to heavy rainfall. According to the normal trend depicted in Figure 9, as time progresses, especially on rainy days, the population's movement tends to decrease, resulting in a corresponding decrease in GPS data. However, it is noteworthy that during the time span from 22:30 on October 12th to 5:00 on the 13th, there is an abnormal increase in GPS data, particularly reaching a maximum difference exceeding 1000 at 1:00 in the morning. Concurrently, based on the river water level variation graph in Figure 3, the river water level rapidly increases from 17:00 on the 12th and reaches its peak at 2:00 on the 13th, closely corresponding to the abnormal time and peak time of GPS data. It is reasonable to infer that a flood occurred during this period, accompanied by a significant population displacement in the early morning hours of the 13th.

The subsequent spatial analysis of the flood will be conducted within this specific time frame.

（3）Spatial Variation

Based on the flood time analysis, the calculation of the grid results and abnormal distribution of GPS data during the flood period are shown in Figure 10.

According to the results of the GPS grid data, there are a total of 175 grids with abnormal GPS data. Among them, 52 abnormal grids are distributed individually, constituting approximately 30% of the total abnormal grids. The remaining 123 grids are adjacent, making up about 70% of the total abnormal grids, primarily concentrated in the circled regions.

As depicted in Figure 11, the overlay of flood extent, rivers, and shelters opened during the flood period reveals a noticeable correlation between adjacent abnormal grids and known flood areas, either adjoining or overlapping. Moreover, these regions are traversed by rivers. Particularly noteworthy is the concentration of abnormal grids near the flooded areas where shelters are located. This could be attributed to the fact that most people transitioning from flood-affected areas to shelters pass
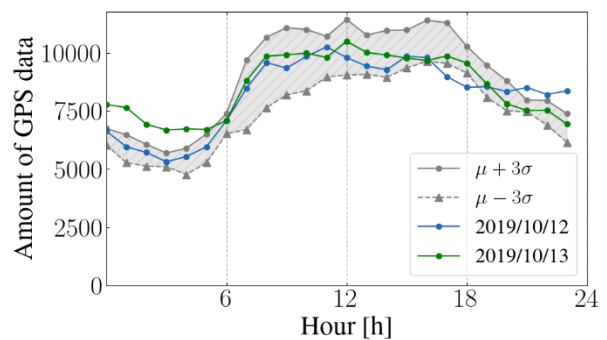

Figure 9 12th and 13th GPS data per hour with normal ranges

Table4 Result of calculation of GPS data range per hour on normal date compared with 12th and 13th

$\mu + 3\sigma$	$\mu - 3\sigma$	Hour	2019/10/12	Value	2019/10/13	Value
6747.137	6045.363	0	6636	0	7774	1
6479.969	5277.531	1	5963	0	7648	1
6067.211	5134.289	2	5717	0	6928	1
5695.492	5100.508	3	5319	0	6683	1
5901.805	4776.695	4	5544	0	6727	1
6511.829	5275.171	5	5965	0	6705	1
7388.622	6520.378	6	7085	0	7088	0
9687.441	6705.059	7	8471	0	8812	0
10663.92	7643.083	8	9572	0	9849	0
11071.79	8188.71	9	9340	0	9912	0
10993.49	8363.007	10	9838	0	9975	0
10703.37	8959.626	11	10250	0	9797	0
11424.29	9034.213	12	9786	0	10489	0
10758.33	9072.169	13	9421	0	10006	0
10951.49	8941.512	14	9272	0	9902	0
10975.53	9347.47	15	9852	0	9766	0
11386.11	9626.895	16	9785	0	9666	0
11287.76	9542.245	17	8973	1	9856	0
10269.12	9127.883	18	8516	1	9556	0
9458.922	8087.078	19	8542	0	8657	0
8790.206	7498.294	20	8330	0	7803	0
7971.024	7461.476	21	8507	1	7521	0
7948.863	6894.137	22	8204	1	7531	0
7376.843	6148.657	23	8366	1	6935	0

through positions connected to the flood edge and adjacent to shelters. It may also be due to the effects of transportation disruption, population evacuation, etc. caused by flooding. This all illustrates the close association between the distribution characteristics of abnormal GPS data and flood events. Spatial analysis and visualization play a significant role in clearly identifying the areas affected by the flood.

5. Discussion

(1) Advantages

This study demonstrates that by solely relying on the detection of abnormal changes in GPS data, it is possible to accurately determine the time and area of flood disasters. Compared to the use of satellite and drone data, GPS data acquisition is more convenient in terms of time and area, enabling rapid and precise detection of disaster occurrences. Furthermore, GPS data can also detect the overall movement direction of populations during natural disasters, which provides valuable assistance in population evacuation and rescue efforts. Additionally, the findings of this study can offer valuable guidance for urban planning and development.

(2) Limitations

The GPS data used in this study was sourced from a single company and does not cover every single person within Nagano City, so there are limitations in the amount of data and data accuracy; these limitations prevent accurate measurement of population change and restrict calculations using smaller grid sizes. This is because the time interval was initially set to 6 hours in order to determine the date of the flooding event, which can be relatively large and may have an impact on the accuracy of the results. Furthermore, this study relied on GPS location data from mobile phones, overlooking situations where populations may be unable to move during major natural disasters. By using the normal distribution model, it is possible to quantitatively determine outliers within a statistical framework, which provides a basis for accurate localization of outliers. However, we also need to be aware of the limitations as the actual distribution of the data may not strictly follow the normal distribution.

(3) Conclusion

In this study, a comprehensive analysis of GPS data during flood events successfully determined the timing and affected flood area. Spatial analysis and visualization techniques were employed to describe the distribution of abnormal GPS data during the flood time. The GPS data predominantly concentrated near rivers, adjacent to flood-prone regions, indicating a close correlation between GPS data abnormal and flood events.

The significance of this study lies in emphasizing the potential value of GPS data in monitoring and analyzing flood events. Our study not only provides methodologies for understanding the association between GPS data and floods but also lays the groundwork for future similar studies.

Future study endeavors could delve deeper into the causal relationships between GPS data and flood events, refine models for enhanced predictive accuracy, and consider the influence of
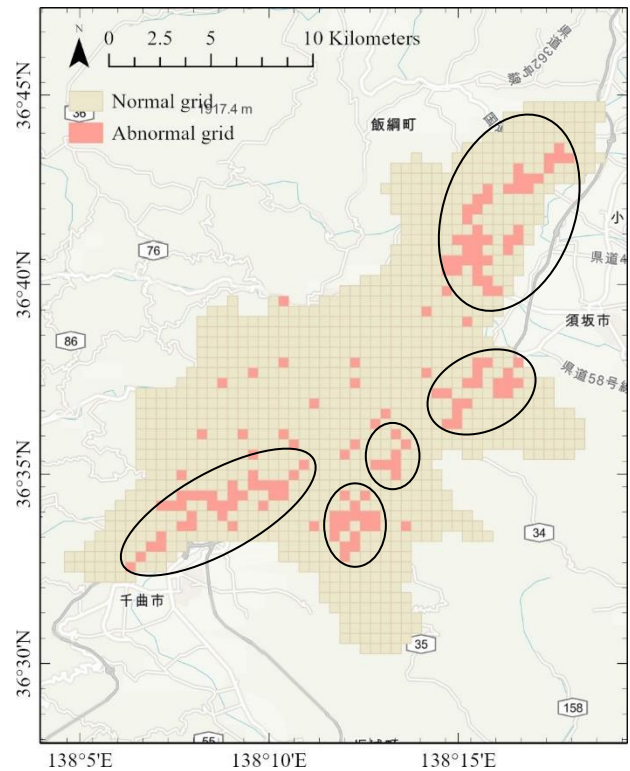

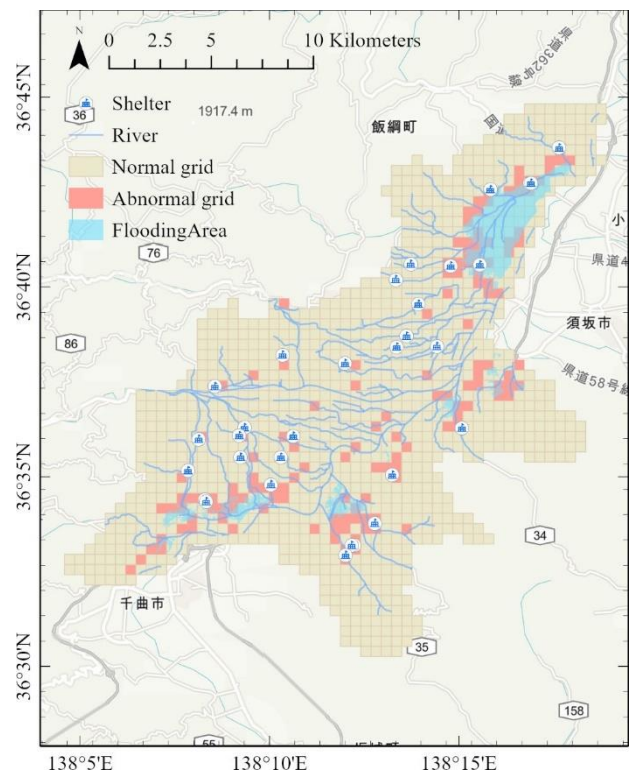Figure 10 Results and distribution of abnormal grids

Figure 11 Overlay analysis of abnormal grids

other environmental factors on GPS data. In disaster preparedness, it is crucial to fully leverage GPS data, integrating it with other data sources and scientific methods to enhance urban resilience against natural disasters. The establishment of a more intelligent and efficient disaster management system will contribute to providing residents with safer and more reliable living conditions.

Acknowledgments

References

1) P. Hu, Q. Zhang, P. Shi, B. Chen and J. Fang: Flood-induced mortality across the globe: Spatiotemporal pattern and influencing factors, Sci. Total Environ. Vol. 643, pp. 171 ,2018.

2) J. S. Cabrera and H. S. Lee: Flood risk assessment for Davao Oriental in the Philippines using geographic information system-based multi-criteria analysis and the maximum entropy model, J. Flood Risk Manag. Vol. 13, No. 2, 2020.

3) M. Higashino and H. G. Stefan: Variability and change of precipitation and flood discharge in a Japanese river basin, J. Hydrol. Reg. Stud. Vol. 21, pp. 68, 2019.

4) J. Park, H. Kim, S.-Y. S. Wang, J.-H. Jeong, K.-S. Lim, M. LaPlante and J.-H. Yoon: Intensification of the East Asian summer monsoon lifecycle based on observation and CMIP6, Environ. Res. Lett. Vol.15, No.9, pp.0940b9, 2020.

5) S. Ohtsuka, Y. Sato, T. Yoshikawa, T. Sugii, T. Kodaka and K. Maeda: Levee damage and revetment erosion by the 2019 Typhoon Hagibis in the Chikuma River, Japan, Soils Found. Vol. 61, No. 4, pp.1172, 2021.

6) K. Yamada and M. Kuribayashi: Topographic effect on heavy rainfall caused by Typhoon Hagibis (2019) in Nagano, Japan, Sola advpub, Vol.17A, 2021.

7) F. Nakai, S. Nakamura and K. Takenouchi: COMMUNITIES' DISASTER PREPAREDNESS PROMOTED EVACUATION: A CASE STUDY OF NAGANO CITY DAMAGED BY THE CHIKUMA RIVER FLOODS CAUSED BY TYPHOON HAGIBIS, J. JSCE Vol.10, No.1, pp.56, 2022.

8) T. Higashino, H. Yamaguchi, A. Hiromori, A. Uchiyama and K. Yasumoto: Edge Computing and IoT Based Research for Building Safe Smart Cities Resistant to Disasters, in 2017 IEEE 37th International Conference on Distributed Computing Systems (ICDCS) (2017) pp. 1729.

9) N. Bharosa, J. Lee and M. Janssen: Challenges and obstacles in sharing and coordinating information during multi-agency disaster response: Propositions from field exercises, Inf. Syst. Front. Vol. 12, No. 1, pp. 49, 2010.

10) S. A. Mohamed: Application of satellite image processing and GIS-Spatial modeling for mapping urban areas prone to flash floods in Qena governorate, Egypt, J. Afr. Earth Sci. Vol. 158, No. 103507, 2019.

11) S. Skakun, N. Kussul, A. Shelestov and O. Kussul: Flood Hazard and Flood Risk Assessment Using a Time Series of Satellite Images: A Case Study in Namibia, Risk Anal. Vol. 34, No. 8, pp. 1521, 2014.

12) A. Tariq, H. Shu, A. Kuriqi, A. Siddiqui, A. S. Gagnon, L. Lu, N. T. T. Linh and Q. B. Pham: Characterization of the 2014 Indus River Flood Using Hydraulic Simulations and Satellite Images, Remote Sens. Vol. 13, No. 11, pp. 2053, 2021.

13) B. Tellman, J. A. Sullivan, C. Kuhn, A. J. Kettner, C. S. Doyle, G. R. Brakenridge, T. A. Erickson and D. A. Slayback: Satellite imaging reveals increased proportion of population exposed to floods, Nature Vol. 596, No. 7870, pp. 80, 2021.

14) H. S. Munawar, A. W. A. Hammad and S. T. Waller: Remote Sensing Methods for Flood Prediction: A Review, Sensors Vol. 22, No. 3, pp. 960, 2022.

15) T. Horanont, A. Witayangkurn, Y. Sekimoto and R. Shibasaki: Large-Scale Auto-GPS Analysis for Discerning Behavior Change during Crisis, IEEE Intell. Syst. Vol. 28, No. 4, pp. 26, 2013.

16) H. Huang and S. Guo: Smartphone Based Emergency Communication. in Big Data in Emergency Management: Exploitation Techniques for Social and Mobile Data, ed. R. Akerkar (Springer International Publishing, Cham, 2020) pp. 131.

17) S. Puttinaovarat and P. Horkaew: Internetworking flood disaster mitigation system based on remote sensing and mobile GIS, Geomat. Nat. Hazards Risk Vol. 11, No. 1, pp. 1886, 2020.

18) X. Zhao, Y. Xu, R. Lovreglio, E. Kuligowski, D. Nilsson, T. J. Cova, A. Wu and X. Yan, Transp. Res. Part Transp. Environ. Vol. 107, No. 103277, 2022.

19) K. Ravikumar and A. RajivKannan: Estimating wildfire evacuation decision and departure timing using large-scale GPS data, Multimed. Tools Appl. Vol. 79, No. 5, pp. 3929, 2020.

20) N. D. Nath, C.-S. Cheng and A. H. Behzadan: Drone mapping of damage information in GPS-Denied disaster sites, Adv. Eng. Inform. Vol. 51, No. 101450, 2022.

21) T. Yoshida, K. Hiroi, Y. Yamagata and D. Murakami: Verification on Evacuation of Flood Disaster by Using Gps: Case Study in Mabi, Japan 2018, in IGARSS 2019 - 2019 IEEE International Geoscience and Remote Sensing Symposium. pp. 5633, 2019.

22) A. Rout, S. Nitoslawski, A. Ladle and P. Galpern: Using smartphone-GPS data to understand pedestrian-scale behavior in urban settings: A review of themes and approaches, Comput. Environ. Urban Syst. Vol. 90, No. 101705, 2021.

23) S. Z. Ziv and Y. Reuveni: Flash Floods Prediction Using Precipitable Water Vapor Derived From GPS Tropospheric Path Delays Over the Eastern Mediterranean, IEEE Trans. Geosci. Remote Sens. Vol. 60, No. 1, 2022.

24) H. Desalegn and A. Mulu: Mapping flood inundation areas using GIS and HEC-RAS model at Fetam River, Sci. Afr. Vol. 12, No. e00834, 2021.

25) T. Manyangadze, E. Mavhura, C. Mudavanhu and E. Pedzisai: Flood inundation mapping in data-scarce areas: A case of Mbire District, Geo Geogr. Environ. Vol. 9, No. 1, pp. e00105, 2022.

26) C. N. Riastama, I. M. Anjasmara and P. Maulida: Monitoring Land Subsidence and its Effect on Surabaya Coastal Inundation by Utilizing GPS Campaigns Data, IOP Conf. Ser. Earth Environ. Sci. Vol. 1127, No. 1, pp. 012002, 2023.

27) M. Hadi, F. Yakub, A. Fakhrurradzi, C. Hui, A. Najiha, N. Fakharulrazi: Designing Early Warning Flood Detection and Monitoring System via IoT, A. Harun, Z. Rahim and A. Azizan, IOP Conf. Ser. Earth Environ. Sci. Vol. 479, No. 1, pp. 012016, 2020.

28) R. Imam, M. Pini, G. Marucco, F. Dominici and F. Dovis: Data from GNSS-Based Passive Radar to Support Flood Monitoring Operations, in 2019 International Conference on Localization and GNSS (ICL-GNSS). pp. 1, 2019.

29) G. S. Ogato, A. Bantider, K. Abebe and D. Geneletti: Geographic information system (GIS)-Based multicriteria analysis of flooding

hazard and risk in Ambo Town and its watershed, J. Hydrol. Reg. Stud. Vol. 27, No. 100659, 2020.

30) A. M. Vinod, D. Venkatesh, D. Kundra and N. Jayapandian, in Second International Conference on Image Processing and Capsule Networks, eds. J. I.-Z. Chen, J. M. R. S. Tavares: Natural Disaster Prediction by Using Image Based Deep Learning and Machine Learning, A. M. Iliyasu and K.-L. Du (Springer International Publishing, Cham, 2022) pp. 56, 2022.

31) M. Ghahramani, M. Zhou and G. Wang: Urban sensing based on mobile phone data: approaches, applications, and challenges, IEEECAA J. Autom. Sin. Vol. 7, No. 3, pp. 627, 2020.

32) B. Hong, B. J. Bonczak, A. Gupta and C. E. Kontokosta: Measuring inequality in community resilience to natural disasters using large-scale mobility data, Nat. Commun. Vol. 12 No. 1, pp. 1870, 2021.